Purging of deleterious variants in Italian founder populations with extended autozygosity — Source link ⧉

Massimiliano Cocca, Marc Pybus, Pier Francesco Palamara, Erik Garrison ...+10 more authors

Institutions: University of Trieste, Pompeu Fabra University, Harvard University, Wellcome Trust ...+2 more institutions

Related papers:

- Accumulation of Deleterious Mutations in Landlocked Threespine Stickleback Populations.

- A survey of functional genomic variation in domesticated chickens

- Ancestry-Dependent Enrichment of Deleterious Homozygotes in Runs of Homozygosity

- Are common disease susceptibility alleles the same in outbred and founder populations

- Exome sequencing identifies high-impact trait-associated alleles enriched in Finns

Purging of deleterious variants due to drift and founder effect in Italian populations with extended autozygosity

Massimiliano Cocca[1], Marc Pybus[2], Pier Francesco Palamara[3], Erik Garrison[4], Michela Traglia[6], Cinzia F Sala[6], Sheila Uiivi[5], Yasin Memari[4], Anja Kolb-Kokocinski[4], Shane McCarthy[4], Richard Durbin[4], Paolo Gasparini[1,5], Daniela Toniolo[6], Nicole Soranzo [4,7], Vincenza Colonna[8]*

1. Department of Medical, Surgical and Health Sciences, University of Trieste, 34100 Trieste, Italy
2. Institut de Biologia Evolutiva (UPF-CSIC), Universitat Pompeu Fabra, Barcelona, Spain, 08003
3. Harvard T. H. Chan School of Public Health, 02115 Boston, MA.
4. Human Genetics, Wellcome Trust Sanger Institute, Genome Campus, Hinxton, CB10 1HH
5. Medical Genetics, Institute for Maternal and Child Health IRCCS "Burlo Garofolo", 34100 Trieste, Italy
6. Division of Genetics and Cell Biology, San Raffaele Scientific Institute, Milano,Italy
7. Department of Haematology, University of Cambridge, Hills Rd, Cambridge CB2 0AH
8. National Research Council, Institute of Genetics and Biophysics, Naples, Italy

*Correspondence to:

Vincenza Colonna
Consiglio Nazionale delle Ricerche
Istituto di Genetica e Biofisica "Adriano Buzzati-Traverso"
Via Pietro Castellino 111
80131 Napoli - IT

tel +39 081 6132 254
fax +39 081 6132 706
email vincenza.colonna@igb.cnr.it

Abstract

Purging through inbreeding occurs when consanguineous marriages increases the rate at which deleterious alleles are present in a homozygous state. In this study we carried out low-read depth (4-10x) whole-genome sequencing in 568 individuals from three Italian founder populations, and compared it to data from other Italian and European populations from the 1000 Genomes Project. We show extended consanguinity and depletion of homozygous genotypes at potentially detrimental sites in the founder populations compared to outbred populations. However these patterns are not compatible with the hypothesis of consanguinity driving the purging of highly deleterious mutations according to simulations. Therefore we conclude that genetic drift and the founder effect should be responsible for the observed purging of deleterious variants.

35

40

45

50

Introduction

Population genetics theory and empirical evidence from model organisms predict that
deleterious variants are purged by selection at a rate proportional to their fitness effect and the
effective population size[1]. However, evidence for similar genetic load in populations that underwent
bottlenecks and constant size populations shows that selection is equally effective regardless of
demography, and therefore a reduction in population size has no effect on the population's genetic
load[2,3,4]. Nevertheless, other demographic factors can affect the efficacy of selection. Inbreeding
depression is the reduction in average population fitness due to higher level of homozygosis than
expected under Hardy-Weinberg equilibrium. Increased homozygosity can lower fitness either by
reducing the heterozygous genotypes at loci with heterozygous advantage, or by increasing the rate
of homozygosity for partially recessive detrimental mutations[5]. This last case exposes deleterious
mutations to selection, driving their purging from the population increasing the effectiveness of
selection.[6,7,8] In cases of systematic inbreeding due to non-random mating (as is the case of small
consanguineous populations), purging can work even for mildly deleterious alleles. However, purging
is effective only for lethal or semilethal alleles in the context of as opposed to cases of panmictic
inbreeding (i.e. inbreeding due to finite size of the populations) and drift[9].

Consanguineous marriages result in substantial deviation from Hardy-Weinberg equilibrium due to
increased autozygosity, which can cause deleterious recessive variants to be present in a
homozygous state. While autozygosity is associated with higher rate of disorders (congenital, late
onset, infertility, miscarriage, infant mortality and morbidity) in consanguineous populations[10–14], it

also provides an opportunity for selection to act by purging exposed deleterious phenotypes,

75   eventually reducing the burden of homozygous deleterious genotypes[8].

Purging causes less fit individuals to be eliminated, ultimately increasing the population's fitness. Indeed, in some species inbreeding caused by a bottleneck has been shown to have beneficial effects, for instance by promoting the invasiveness of some species of ladybirds[15] or removing highly deleterious variants in mountain gorillas[16]. In humans, consanguineous couples experience higher

80   fertility than non-consanguineous couples[12,17,18], but this has been associated with causes other than purging of deleterious variants, such as social factors (e.g. younger maternal age at first birth), reproductive compensation[12], and the negative effects of outbreeding, including the break up of co-adapted gene complexes, and the increase of maternal-foetal incompatibility[18]. Little is known about how inbreeding might play a role in the improved fecundity of consanguineous couples.

85   In this study we investigated whether autozygosis has had a role in the purging of deleterious mutations in three Italian founder populations with different demographic histories[19–21] by comparing them with outbred Italian and European populations. We show evidence for a depletion of homozygous genotypes at putatively detrimental sites in all the three populations. The presence of this effect in multiple founder populations with high rates of consanguinity suggested that

90   inbreeding might have had a role in accelerating purging of deleterious mutations. However, according to simulated results consanguinity could not be responsible for the observed purging, therefore we conclude that genetic drift and the founder effect have driven the observed purging of deleterious variants from these isolated human populations.

95   Results

Whole genome sequence of isolates identified 21M variable sites

We carried out low-read depth whole-genome sequencing (average 6x, Table S1) in 568 unselected individuals from three populations from the Italian network of genetic isolates (INGI), namely Val Borbera (VBI), Carlantino (CAR) and Friuli Venezia

100   Giulia (FVG). Of these, FVG is further subdivided in 4 different villages, namely Erto (FVG-E), Illegio (FVG-I), Resia (FVG-R) and Sauris (FVG-S) (Figure 1a and Table S2). After stringent quality control (Methods), we identified a total of 21,244,190 variable sites. We further compared genetic variability of the isolates with populations representative of the general Italian and European population, namely 98 Tuscans

105   (TSI) and 85 Utah Residents with Northern and Western European ancestry (CEU) from the 1000 Genomes Project (TGP)Phase 1 data set[22,23] (Figure 1a). The isolate call sets were generated using the same variant calling and QC pipelines employed by the TGP project, so the two variant datasets were merged to generate a final set of 46,281,641 variable sites including sites variable both in isolates and TGP. To

110   verify the validity of this approach, we estimated concordance of genotypes at 298k variable sites on chromosome 22 within the merged call set with those obtained by simultaneously calling isolates and the TGP. We found a median non-reference genotype discordance of 1.55% and 3.8% for SNPs and INDELs, respectively (Table S3), suggesting that merging the two call sets is a viable approach.

115   We investigated genetic relationship among individuals of the three isolates, TSI and CEU using a random set of 281k variable chromosome 22 sites spanning all frequency ranges. A previous exploration of VBI and FVG was limited to low-resolution SNP array data which is not informative for rare, private and novel genetic

variation[19,20] while the genetic structure of CAR has not been described before. In a
120   principal component analysis, two FVG villages (FVG-R and FVG-S) appeared to be
distinct from the other populations along the first three components. Further, VBI
and CAR separated from CEU and TSI on the fourth component (Figure S1). In
admixture analyses, FVG-R and FVG-S separated from other populations already at
K=4 clusters, although the most likely number of clusters was 10 (Figure S2). These
125   results confirm earlier results based on SNP array data from the entire FVG sample[20],
and are thus not related to the sampling strategy used in this study. Because of this
sub-structuring, when relevant FVG villages were considered separately for
subsequent analyses. CAR, described here for the first time, clusters with VBI and
other reference populations (TSI and CEU) along the first two components and with
130   VBI along the 3rd and 4th component (Figures S1 and S2).

Using a different data set of variants obtained by jointly calling the TGP and
isolated populations cohorts that do not include CAR, we evaluated FST distance
between pairs of populations (Table S4). As shown in previous publications[20] the
between-populations pairwise Fst values of the FVG villages were extremely high.
135   The overall mean between pairs of villages is 2%, which is substantially higher than
the Fst values between the villages and the other populations, which range from 1-
1.5%. Other pairwise Fst were below .5%.

<p style="color:red; text-align:center;">Long term isolation and diffused homozygosity in isolated populations</p>

140   FVG[20] and VBI[21,19] are located in two mountain regions of North Italy that were in
the past poorly connected to neighbouring areas. In addition to geographical
isolation, FVG villages experienced linguistic isolation due to their use of very

different dialects. In the 14th century people moving from the area of Naples migrated some 300 km to found the CAR population, which experienced isolation

145   due to differences in dialect with surrounding communities and poor connection to its parent population. The historical isolation experienced by isolates causes systematic inbreeding, which is expected to result in greater genetic homogeneity and homozygosity as compared to reference population. We investigated this hypothesis using several approaches.

150   First, we calculated relatedness between pairs of individuals using two independent measures, namely pedigree-based and genome-based kinship. Pedigree based kinship represents the expected fraction of the genome shared that is identical by descent (IBD) and was calculated from available genealogical records dating back to the 17th century for VBI [21,24] , records collected during sampling of

155   DNA for FVG, and from private genealogical collections available for CAR.   Genomic kinship is the fraction of the genome which is shared identical by descent and was calculated using genetic data. Pedigree- and genome-based kinship values were highly correlated (Figure S3), however in FVG villages the resolution of pedigree-based kinship was poor because genealogies are incomplete, therefore we focused

160   on genomic based-kinship.

       Genome-based kinship values are significantly higher in isolates than reference populations and average kinship in isolates is always higher than reference populations (Figure 1b; Table S5; two-sample Kolmogorov-Smirnov and Mann-Whitney test p-value in Table S6) . The kinship distributions were highly skewed

165   towards low values in all cases, however maximum values were in the range of 1st degree relationships for isolates, compared to approximately 3rd degree in reference populations (Figure 1b, "All"). When removing one individual per pair from pairs

related to the 1st degree according to pedigree data, we still observed genomic-kinship values in the range of 1st degree in FVG-R and in VBI (Figure 1b, "All

170   Unrelated"). We confirm that the observed differences were not due to different sample sizes, by re-calculating genomic kinship for a subset of 46 random individuals per population (Figure 1b, "46 Unrelated"). Overall, these results not only show that individuals from isolates tend to be more consanguineous than reference populations, but also suggest that consanguinity has systematically

175   occurred in these populations in historical times, and ancestors of 2nd and 3rd degree relatives were in turn the result of consanguineous relationships. Because of this extended consanguinity, we excluded from subsequent analyses one randomly-selected individual from pairs with 1st degree relationships (Table S1)

Having assessed diffused consanguinity in the isolates, we next quantified

180   genome segments which were IBD among pairs of 46 random unrelated individuals per population. In Figure 2a we report the distributions of total extension of IBD per genome (i.e. the sum of single segments). While there was no significant difference between isolates and CEU or TSI in the total IBD distributions (two-sample Kolmogorov-Smirnov test p-value >0.01, Table S7) FVG villages displayed higher

185   total IBD sharing on average (Figure S4 and Table S7). These differences were more evident when contrasting cumulative distributions of total IBD (Figure 2c and Table S7): in FVG villages 95% of the individuals shared 337-461(+/-85-123)Mb compared to 122-157(+/-8-45)Mb in other isolates and reference populations. Considering an accessible genome size of 2.5Gb[23], this would indicate that individuals in FVG

190   villages share between 13% and 18% of their genomes, *versus* 5-6% in other populations, corroborating evidence for extended consanguinity in the isolates.

Finally, we investigated allele sharing within an individual by identifying genomic segments with contiguous genotypes in homozygosity (Runs Of Homozygosity, ROH) in each individual. We report in Figure 2b the distributions of the total length of ROH

195 (i.e. the sum of single segments) per individual. With the exception of CAR, ROH extension was significantly higher in isolates compared to CEU and TSI (two-sample Kolmogorov-Smirnov test p-values in Table S7), suggesting increased homozygosity in isolates. This is also evident when comparing cumulative distributions of total ROH in 46 randomly selected individuals per population (Figure 2d, Table S7): 95% of

200 individuals in FVG villages and VBI had between 163-209(+/-30-43)Mb of genome in homozygosis compared to less than 100(+/-10-15)Mb in the outbred reference populations. These figures suggest 5-8% of the genome is in homozygosity in isolates (except CAR) while only 3-4% is in CEU and TSI.

When ROHs segments were classified according to their length[25], we observed a

205 greater prevalence of medium and long ROHs in isolates (and especially FVG-R and FVG-S) than in CEU and TSI (Figure S5). This condition is consistent with the presence of extended consanguinity or very recent admixture; both cases apply to the isolates under study here, for which isolation (either geographical or linguistic) was a past condition that is no longer met.

210

Isolates experienced genetic drift and a recent decrease of the effective population size

Isolated populations are expected to be more greatly subjected to the effect of genetic drift compared to outbred populations, therefore we investigated to what

215 extent genetic drift acted on the populations in this study. We used a method based

on inference from genomic segments that are shared IBD which enables the exploration of very recent fluctuations in effective population size[26] . Low coverage and computational phasing are likely to affect the accuracy of IBD detection methods, occasionally breaking down long IBD segments into shorter ones and thus

220   potentially creating the artefactual effect of a population expansion. Despite this potential confounding, our analysis displayed clear patterns of overall lower effective population size estimates in isolates compared to reference populations (Figure 3). In the last fifty generations (approximately last 1500 years) we observed a population size contraction in FVG villages compared to CEU and TSI, which appear unaffected

225   by the recent trends towards expansion of other European populations[27,28]. Such abundant sharing of long haplotypes co-inherited from recent common ancestors during a recent population contraction provides further evidence for genetic drift that extended until the very recent centuries in these isolated groups. CAR and VBI have a less pronounced trend of contraction compared to FVG, however they still

230   have smaller effective population sizes compared to TSI and CEU. We therefore conclude that isolates experienced more genetic drift compared to reference populations.

<p style="text-align:center; color:red">Depletion of putatively detrimental sites in isolates</p>

235   To test the hypothesis that autozygosity contributes to the purging of deleterious mutations through exposure of detrimental alleles to purifying selection, we determined the incidence of homozygous detrimental genotypes and measured the efficiency of purifying selection in isolates compared to reference populations.

To compare allele frequencies we used a different data set of variants obtained
by jointly calling the TGP and isolated populations cohorts and do not include CAR.
Starting from this data set we selected 322 individuals (46 randomly selected
unrelated individuals per population) for which we identified 12,344,818 variable
sites. Of these, 10,917,001 sites had information on the ancestral state of the alleles
and were considered for further analyses. After determining derived allele
frequencies (DAF) per each population we evaluated incidence of derived allele
causing missense (356,155 sites), synonymous (229,529 sites), or loss of function
(LoF, 4,286 sites)[29] consequences. Alleles determining missense (and some time
synonymous[30]) consequences introduce changes to the coded protein that might
alter the protein structure, whereas LoF alleles completely disrupt the protein
function. We used a million sites annotated as intergenic as a proxy for neutrality in
comparisons.

With few exception, we observed significantly fewer derived alleles counts per
individual in FVG and VBI compared to reference populations at synonymous and
intergenic sites, whereas derived allele counts at missense and LoF sites was overall
comparable (Figure 4a, Wilcoxon rank sum test p-values in Table S8). We then
evaluated how often putatively detrimental alleles are found in homozygosis by
counting the number of homozygous derived genotypes per individuals. Isolates had
significantly higher rates of homozygous derived genotypes at neutral and
synonymous sites (Figure 4b, Table S8) compared to reference populations, in
accordance with the general homozygosity trend reported in a previous section.
However, with one exception (FVG-R), we found no significant differences in the
rates of homozygosity at missense and LoF deleterious sites between the reference
and isolate populations. This is indicative of an overall depletion of homozygous
genotypes at deleterious sites in the isolates, which, along with the comparatively

11

265   high rates of homozygosis at neutral alleles, supports the hypothesis the hypothesis

that deleterious alleles have been purged through inbreeding in the isolates

We therefore used a recently proposed metric ($R_{X/Y}$)[2,4] to assess whether

selection has been more effective in isolates compared to reference populations. The

metric $R_{X/Y}$ contrasts frequencies of alleles between pairs of populations and

270   measures their accumulation in one population compared to the other: a value of 1

indicates that the two populations have comparable number of mutations per

individual, whereas values lower than 1 indicate a depletion in population X and

values higher than 1 indicate a depletion in population Y. We compared $R_{X/Y}$ at

intergenic, synonymous, missense, and LoF variants in isolates and reference

275   populations using derived allele counts of 46 randomly selected individuals per

population.

Overall, $R_{X/TSI}$ values for all functional categories were closer to one compared to

$R_{X/CEU}$ ones, reflecting the greater similarity of isolates to TSI than to CEU (Figure 5).

With the exception of VBI and FVG-I, in all comparisons involving intergenic and LoF

280   sites $R_{X/Y}$ was not significantly different from one, however for LoF $R_{X/Y}$ values were

less accurate, because of the low number of sites considered. In most cases, $R_{X/Y}$ at

synonymous and intergenic sites was similar and a trend of diminishing $R_{X/Y}$ is visible

among intergenic, synonymous and missense sites. From a populations perspective,

for VBI both $R_{X/CEU}$ and $R_{X/TSI}$ were always significantly less than one at all functional

285   categories, whereas for FVG villages patterns are less simple. Overall, besides details

of single categories and populations, we observed many cases in which $R_{X/Y}$ was

significantly lower than one in isolates especially at sites with deleterious functional

consequences (i.e. missense) suggesting that isolates were depleted of putatively

detrimental alleles. While for intergenic sites $R_{X/Y}$ is almost always significantly equal

290   to 1, at other categories it is often significantly <1 suggesting more efficient

selection in isolates compared to reference population. These patterns could possibly

arise due to the founder effect, the genetic drift and the purging effect of inbreeding

alongside strong selection coefficients for highly disruptive mutations.

Simulations support the observed depletion of highly deleterious homozygous genotypes but fail to see any effect of inbreeding

We evaluated expectations to observe purging in simulated data under a range

of demographic scenarios, natural selection intensities and models. A population

isolate was simulated to arise from an European-like population at 160, 60 or 20

300   generations ago (generation time 25 years), and to evolve to present time under five

demographic models (continued bottleneck, serial founder effect, bottleneck plus

linear expansion, bottleneck plus instantaneous expansion and bottleneck plus linear

reduction; Figure S6) and three different values of average kinship (0, 0.002 and

0.01). We forward-in-time simulated genomic data by mimicking features of exomes

305   spanning 115 kbp (Methods). Mutations were assumed to be deleterious ¾ of the

time in exons and ½ in UTRs under six selection coefficients (s = -0.2, -0.1, -0.05, -

0.01, -0.005 and -0.001). Each scenario was replicated 500 times. We found purging

to be more effective in the bottleneck plus expansion (Figure S7) and thus for this

model we further explored a range of bottleneck intensities (effective population

310   size, Ne, during the bottleneck = 15, 25 and 50 and bottleneck duration 1 to 25

generations in steps of 5, Table S9). Demographic parameter choice was a

compromise between computational feasibility and similarity to the demography of

the isolates under study, its main purpose being to explore properties of purging rather than to perfectly fit isolate demography.

315   Purging was calculated in a sample of 50 individuals as the fold change between present and past (at founding event) number of recessive deleterious homozygous genotypes per individual. A negative fold change indicates a reduction of deleterious homozygous genotypes, as is expected in the case of purging. Results in Figure 6 (also see Figure S8) show that: (i) under neutrality ($s = 0$) no purging is seen in all

320   three models; (ii) for mildly deleterious mutations ($s = 0.01$) purging is almost complete under dominance, moderate for additive models but not observed under recessive models; and (iii) for highly deleterious mutations ($s = 0.1$) purging of homozygous recessive deleterious genotypes is also seen under recessive models.

Overall, these simulations suggest that the selection coefficient and dominance

325   model have a major effect on purging and that purging is possible for highly deleterious recessive mutations. While it is difficult to make assumptions on the inheritance model of missense and synonymous variants, a recessive model and a strong selection coefficient are highly plausible for LoF[29]. We therefore conclude that simulations support the observed depletion of highly deleterious homozygous

330   genotypes observed at LoF sites. Nevertheless, our set of simulations does not explain the role of consanguinity as the effect of kinship is negligible (Figure 6). This may be due to the imperfect fit of the demographic parameters used for simulations to the isolates studied here. A more comprehensive analysis will be required to fully understand this aspect.

335

Discussion

Inbreeding consists of mating between closely related individuals. Chromosome pairs of inbred offspring share segments that are identical by descent more often than expected by chance, and consequently large portions of the genome in inbred individuals are in homozygosis. Inbred offspring

340 undergo inbreeding depression, the phenomenon by which the overall fitness of the population is reduced due to higher levels of homozygosity than Hardy-Weinberg expectations, including the rise of homozygous detrimental mutations. However, inbreeding depression cannot be maintained permanently, as eventually the genetic load caused by the rise of the frequency of detrimental mutations is offset by an increased efficiency of selection as inbreeding drives higher rates of homozygosis at

345 recessive deleterious alleles, increasing the chance that these alleles manifest a phenotype that may be selected upon in a process known as genetic purging. Therefore, in the long term inbreeding can have positive effects on fitness. While this was demonstrated to be the case for other species (e.g.[15,16]), it has never been demonstrated for humans[2].

We decided to assess if genetic purging has occurred in three Italian isolated populations which are

350 likely to feature high rates of inbreeding. By performing the analysis of whole genome data we first demonstrated the occurrence of (i) diffused consanguinity, (ii) extended regions of autozygosity and (iii) small effective population sizes until recent times, showing that indeed the three populations are genetic isolates and the genomes of their members are more homogeneous than those of representatives of outbred European and Italian populations. Secondly, we compared allele

355 frequencies between isolates and reference populations at putatively detrimental and neutral sites and showed a depletion of homozygous genotypes of putatively deleterious mutations in the isolates. Furthermore, according to a statistic that measures the efficacy of selection at removing deleterious genotypes, population isolates have fewer deleterious allele at detrimental sites than neutral ones.

360   Following this evidence we then used simulations to understand if the depletion of homozygous deleterious genotypes could have been the result of purging using simulations. In accordance with other published studies[4], our simulations showed that a reduction of homozygous deleterious genotypes is indeed possible after a bottleneck assuming a recessive model and strong selective pressure. However, we did not observe a change in the efficacy of selection when varying the inbreeding

365   coefficient of the simulated population. Therefore we concluded that under the considered simulation scenario, the observed depletion of deleterious homozygous genotypes might be a general effect of the demography compatible with the general loss of rare alleles due to bottlenecks and genetic drift.

        Consanguineous populations represent a model for the effects of systematic

370   inbreeding. Consanguinity can naturally occur for several reasons, including geographical, linguistic and religious isolation. Recently there has been a great interest in exploring the genetic load in populations with different demographic history. Consanguineous populations in this study complement the range of demographic scenarios and here we demonstrate that they provide an excellent

375   model study to understand the interplay between selection, genetic drift and homozygosis in determining the genetic load of human populations.

Methods

Samples individuals and data generation

380   Low coverage whole genome sequence was generated in for 568 individuals belonging to the INGI network. Individuals are from Italian populations form North-West (Val Borbera[21], 225 samples), North-East (Friuli Venezia Giulia[20], 250 samples)

and South-West (Carlantino[20], 93 samples). Sequencing was carried out using

Illumina technology (Genome Analyzer and HiSeq 2000) at the Wellcome Trust

385   Sanger Institute and Beijing Genomics Institute (54 samples from FVG cohort). Data

coverage was 4-10X (Table S2).

The study was reviewed and approved by the following Ethical Committees:

Ethical committee of the San Raffaele Hospital and of the Piemonte Region (VBI),

Ethics approval was obtained from the Ethics Committee of the Burlo Garofolo

390   children's hospital in Trieste (FVG), the local administration of Carlantino, the Health

Service of Foggia Province, Italy, and ethical committee of the IRCCS Burlo-Garofolo

of Trieste (CAR). Written informed consent was obtained from every participant to

the study and all methods were carried out in accordance with the approved

guidelines (Declaration of Helsinki of the World Medical Association).

395

Data processing, variant calling

Genotype calls were produced for each population separately using the following

pipeline. Samtools mpileup (v. 0.1.19)[31] was used for multisample genotype calling

(parameter set: -EDVSp -C50 -m3 -F0.2 -d 40). Variant Quality Score Recalibrator

400   (VQSR) filtering was applied to the raw call data with GATK v.2.5[32] through

VariantRecalibrator module separately for SNVs and INDELs. The filter creates a

Gaussian Mixture Model by looking at annotations values over a high quality subset

of the input call set and then evaluate all input variants. For SNVs we used the

following parameters: I) Annotations: QD, DP, FS, HaplotypeScore, MQRankSum,

405   ReadPosRankSum, InbreedingCoeff II) Training set: HapMap 3.3, Omni 2.5M chip,

1000 Genomes Phase I; III) Truth set: HapMap 3.3 ,Omni 2.5M chip; IV) Known set:

dbSNP build 138. For INDELs we selected: I) Annotations: DP,FS,ReadPosRankSum,MQRankSum; II) Training set: Mills-Devine, 1000 Genomes Phase I, DbSnp v138; III) Truth set: Mills-Devine; IV) Known set: Mills-Devine, dbSNP

410   build 138. For each population the lowest VQSLOD threshold has been chosen according to the output produced by VariantRecalibrator to select the best cut off in terms of specificity and sensitivity of the trained model. For SNPs the minimum VQSLOD values selected are 3.016 (97.3% truth sensitivity threshold), 2.8309 (97.82% truth sensitivity threshold), 1.4512 (98.5% truth sensitivity threshold) for

415   FVG, VBI and CARL cohort respectively. Since INDELs calling and alignment is still more prone to error we used a conservative approach, selecting a sensitivity threshold of 90% for each population. The filter has been applied using GATK's Apply Recalibration module.

To ameliorate the low quality of raw genotyping results based on the low

420   coverage sequencing data we performed several genotype refinement steps on the filtered call set: 1)we used BEAGLEv4.r1230[33] to assign posterior probabilities to all remaining genotypes. 2) SHAPEITv2[34] has been used to phase all genotypes call and 3) IMPUTEv2[35,36] to perform internal imputation in order to correct genotyping errors. Information about Ancestral Allele and allele frequencies from TGP populations have

425   been retrieved from dbSNP v.138[37]. The Variant Effect Predictor v.74[38] provided all consequence annotation as well as Polyphen,Sift and GERP informations.

We merged genotype call set of the INGI populations with low coverage data available from Phase1 of the 1000 Genomes Project[23] in a union using set using bcftools merge[31]. To check if this approach would introduce bias in downstream

430   analyses, we evaluated genotype discordance on chromosome 22 between the union set and a genotype call set in which variants were called simultaneously in all INGI,

bioRxiv preprint doi: https://doi.org/10.1101/022947; this version posted October 12, 2015. The copyright holder for this preprint (which was not certified by peer review) is the author/funder, who has granted bioRxiv a license to display the preprint in perpetuity. It is made available under aCC-BY-NC-ND 4.0 International license.

S*Cocca et al. - Purging of deleterious variants in founder populations*

CEU and TSI populations using the same pipeline described above. Discordance was calculated by comparing the genotypes of the same sample in the two sets and counting cases in which alleles were called differently, e.g. the Ref/Ref_discordance was the proportion of cases where a Ref/Ref genotypes in one set was wrongly called as a Ref/Alt or Alt/Alt in the other set. We details these definitions in the Table S3 caption.

Joint calls from the data set of the Haplotype Reference Consortium

The Haplotype Reference Consortium (HRC.r1) callset was created by merging the data from 20 separate large whole-genome sequencing projects (see http://www.haplotype-reference-consortium.org for details of these cohorts including numbers and average sequencing coverage). The initial set of sites was selected by combining the individual phased SNP callsets from these cohorts. Non-biallelic sites were split into biallelic sites and sites with minor allele count (MAC) >= 5 were selected. Genotype likelihoods (GLs) were extracted from the original alignments (BAM files) using samtools mpileup/bcftools call[31]. Having generated GLs at these sites, further site filtering was performed by removing a set of sites that could be putatively called within cohorts from the likelihoods, but have been filtered out consistently across the initial callsets. The HRC.r1 sites were further filtered sites for which any of the following statements were true: (i) Per-cohort Hardy-Weinberg Equilibrium (HWE) p-value $< 10^{10}$ and cohort is not 1000 Genomes; (ii) Overall inbreeding coefficient < -0.1; (iii) Minor allele frequency (MAF) > 0.1, site called in less than three cohorts, and site not called in 1000 Genomes. Additionally sites found on a selection of common SNP genotyping arrays were reintroduced if they had been filtered by any of these steps. The final site list contains 39,235,157 autosomal sites.

19

In Table S10 we report fractions of sites with p(HWE) <1.0e-4 per population. Allele frequency spectrum for the minor allele is shown in Figure S10.

460

From the initial set of samples collected, some were removed due to low call rate based on putative calls from bcftools based on GLs. A further set of samples were removed to eliminate duplicate samples that had been sequenced across multiple studies, resulting in 32,488 samples in the final set. A new extension of the SNPtools algorithm[39] which takes advantage of pre-existing haplotypes was used to call haplotypes from the GLs. We merged these haplotypes with the pre-existing haplotypes by setting the genotypes of any sites which were only found in the pre-

465

existing haplotypes to be homozygous major allele in the new haplotypes. A development version of SHAPEIT was then used to refine the phasing of the called haplotypes.

Population genetic structure

470

Shared ancestry between populations was evaluated using ADMIXTURE v 1.22 and the number of cluster that better represent the data was established by cross-validation as described in[40]. Each ADMIXTURE run was replicated 5 time using different random seeds. Principal Component Analysis (PCA) analysis was performed using EIGENSOFT [41].

475

Kinship, identical by descent state and runs of homozygosity calculations

Pedigree-based kinship was calculated using the R package Kinship2[42] using genealogical records. For VBI, pedigrees were reconstructed using data of births, marriages and deaths from the 16th century onwards, collected from churches and

city council archives [21,24]. Pedigree data collection was approved by the institutional

480   ethical committee of the San Raffaele Hospital in Milan and by the Regione

Piemonte. Pedigrees of FVG were reconstructed using data collected during sampling

and pedigree data collection was approved by the Ethics Committee of the Burlo

Garofolo children hospital in Trieste (FVG). Pedigrees of CAR were reconstructed

from private data donated to the project and approval was obtained by the local

485   administration of Carlantino, the Health Service of Foggia Province, Italy, and ethical

committee of the IRCCS Burlo-Garofolo of Trieste.

Pedigree-based kinship measures provide the expected value of the amount of

genome shared identical by descent, however recombinations and mutation

introduce variability around the expected values. Genome-based kinship directly

490   accounts for this variability and provide continuous estimates of kinship rather than

pedigree-based point estimates (e.g first-degree kinship vary between 0.25+/-

variability). Pairwise genomic kinship was calculated using KING[43] (options: --kinship

--ibs). A negative genomic kinship coefficient indicates an unrelated pairs and for

practical purpose it is safe to rescale negative kinship values to zero [43]. All analyses

495   except kinship distributions were performed on individuals related at most to 2nd

degree according to pedigree-based kinship.

Segments of identity by descent (IBD) and runs of homozigosity (ROH) were

identified using the refined IBD algorithm implemented in Beagle v4.r1274[44]

(parameters used: ibd=true, window=24000, overlap=7000). All variants with

500   uncalled genotypes were removed, leaving 7,502,857 sites for further analyses. After

discovery we retained IDB and ROH segments with LOD score >5 as threshold to

define a true IBD/ROH segment (default value LOD >= 3). When comparing IBD

sharing, ROH data and allele frequencies populations were randomly down-sampled

to match the size of the smallest village size (FVG-I, 46 unrelated samples) in order

505   to reduce bias from different sample sizes.

Effective population size

Recent effective population size for each population was estimated using the fraction of genome shared IBD by pairs of individuals[26]. After computational phasing, IBD sharing was computed as described in[45]. We initially removed all variants with

510   minor allele frequency less than 1%. We used a publicly available genetic map (b37, Web Resources), using linear interpolation to infer the genetic position of variants that were not found in the map. We then used the GERMLINE[46] software to infer IBD sharing across all pairs of samples, using parameters "-min_m 1 -err_hom 2 -err_het 0 -bits 75 –h_extend -homoz". We computed the density of IBD sharing per genomic

515   region using windows of 0.5 centimorgans (cM), and selected for downstream analysis regions within 5 standard deviations from the genome-wide average, removing regions of unusual sharing, likely due to artifacts or the presence of underlying structural variation. We further imposed a minimum length of 45cM per genomic region to avoid introducing biases due to boundary effects in very short

520   regions. We obtained 27 regions, for a total of ~2050 cM. We computed the fraction of genome shared by the average pair of haploid individuals in each analysed group through segments of length at least 6 cM. We then used the formula: $N=(1-f+\sqrt{1-f})/2uf$ derived in[26], where f is the observed fraction of genome shared IBD and u is the minimum segment length (in Morgans) to infer effective population size

525   (assuming a constant size). We report diploid effective sizes. Standard errors were computed using the weighted jackknife method[46], using the 27 genomic regions. To infer an approximate correspondence between IBD segment cut-off and time, we considered the distribution of IBD segments age in a constant population size.

Assuming a generation time of 30 years[47] a cutoff of 6 cM roughly corresponds to

530　　IBD segments originating in common ancestors living 30*(100/6)=500 years before

present.

$R_{X/Y}$

The metric $R_{X/Y}$ was calculated implementing the formula described in[2,4] and [16]

using the information on derived alleles counts per individual in 46 samples per

535　　population. Variance of $R_{X/Y}$ was obtained by block jackknife procedure as described

in [48]. To avoid biases due to lack of calling and imputation we considered only sites

called as variable in both X and Y populations (shared sites). Information on the

ancestral state of the allele were taken from 1000 Genomes annotations

(http://ftp.1000genomes.ebi.ac.uk/vol1/ftp/phase1/analysis_results/supporting/ancest

540　　ral_alignments/). We used four sets of variants with information on functional

consequences from Ensembl database v. 78 (www.ensembl.org): (i) 136,805 variants

annotated as intergenic, i.e. "in region containing or overlapping no genes that is

bounded on either side by a gene, or bounded by a gene and the end of the

chromosome" according to Sequence Ontology definition (S.O.,

545　　http://www.sequenceontology.org/); (ii) 25,773 missense variants, i.e. "A sequence

variant, that changes one or more bases, resulting in a different amino acid

sequence but where the length is preserved" (S.O.); (iii) 23,242 synonymous, i.e. "A

sequence variant where there is no resulting change to the encoded amino acid"

(S.O.), and (iv) 2,804 loss of function variants described in[29]

550　Simulations

We used SLiM[49] to perform forward-in-time simulation of purging of deleterious

recessive alleles in a small size human isolated population. SLiM allows simulations

of specific genomic structures with different selective pressures acting on them. We simulated a genomic region of 115 kbp containing fifty gene-like structures

555   representative of the average human gene[50] each composed of 8 exons of 150 bp surrounded by 2 UTR regions of 550 bp. We set the recombination rate to 1.6e-8 recombinations/bp/generation, the mutation rate to 1.2e-8 mutations/bp/generation, and generation time was set to 25 years. Mutations were assumed to be deleterious ¾ of the time in exons and ½ in UTRs. Six deleterious selection coefficients were

560   tested independently (s = -0.2, -0.1, -0.05, -0.01, -0.005 and -0.001). Deleterious mutations were assumed to be fully recessive, additive, or dominant.

For the demographic model we simulated an isolated population of European ancestry undergoing a founder event of different intensity in terms of number of individuals and length of the bottleneck (see simulation scheme in Figure S7) and

565   then evolving under an specific demography. Three different split times of the isolate from Europe (160, 60 and 20 generations ago), and five demographies were tested: continued bottleneck, serial founder effect, bottleneck plus linear expansion, bottleneck plus instantaneous expansion and bottleneck plus linear reduction). To mimic isolation we assumed no migration between the isolate and the European

570   population after the split. The European population was simulated under the model described in[51] with a minor modifications: because SLiM does not simulate exponential growth we extrapolated the trajectory of the exponential growth found in Out-of-Africa populations from[51] and increased population effective size every few generations. Finally, in our model the European population separates from the

575   African as described in[51]. To mimic relatedeness we let inbreeding starts one generation after the split between Europe and the isolate using two inbreeding coefficients: one similar to estimates from empirical data (averages among all isolates, f = 0.002, Table S7) and a second one five times bigger (f = 0.01). To use

these inbreeding coefficient in the forward simulator (SLiM), we converted

580   inbreeding coefficient (f) to selfing coefficient (σ) using the formula:

$$f = \sigma/(2(1- \sigma/2))$$

described in (http://darwin.eeb.uconn.edu/eeb348/lecturenotes/inbreeding.pdf).

Each set of parameters and demographies was simulated 500 times and, additionally, we considered groups of 10 replicates together as they were

585   independent chromosomes in order to reduce the variance in the individual recessive load calculation. From every simulated replica we sampled 50 individuals in each of the three populations. In simulations with a final population effective size of less than 50 individuals the whole population was sampled. To speed up computation we used two strategies. First, we removed from simulations the

590   neutrally evolving intergenic and intronic regions, thus mimicking exomic data. Secondly, to avoid repeating the burn-in process, we simulated 500 replicates for Africans and Europeans and saved all the individual genotypes at 200 generations before present (5000 years ago) and we used these population snapshots as genetic pools for the founding nucleus of the isolate while testing different demographic

595   models. We believe that this strategy ensures enough variation for testing properly the different population sizes for the ISO population without having to use a new simulations run from the scratch.

References

600   1. Kimura, M. *Population Genetics, Molecular Evolution, and the Neutral Theory*. (University of

Chicago Press, 1995). at

<http://www.press.uchicago.edu/ucp/books/book/chicago/P/bo3645416.html>

2. Do, R. *et al.* No evidence that selection has been less effective at removing deleterious

mutations in Europeans than in Africans. *Nat. Genet.* **47,** 126–131 (2015).

605   3. Simons, Y. B., Turchin, M. C., Pritchard, J. K. & Sella, G. The deleterious mutation load is

insensitive to recent population history. *Nat. Genet.* **46,** 220–224 (2014).

4. Balick, D. J., Do, R., Cassa, C. A., Reich, D. & Sunyaev, S. R. Dominance of Deleterious Alleles

Controls the Response to a Population Bottleneck. *PLoS Genet.* **11,** e1005436 (2015).

5. Charlesworth, D. & Willis, J. H. The genetics of inbreeding depression. *Nat. Rev. Genet.* **10,**

610   783–796 (2009).

6. Whitlock, M. C. Selection, load and inbreeding depression in a large metapopulation.

Genetics **160,** 1191–1202 (2002).

7. García-Dorado, A. A simple method to account for natural selection when predicting

inbreeding depression. *Genetics* **180,** 1559–1566 (2008).

615   8. Kirkpatrick, null & Jarne, null. The Effects of a Bottleneck on Inbreeding Depression and the

Genetic Load. *Am. Nat.* **155,** 154–167 (2000).

9. Glémin, S. How are deleterious mutations purged? Drift versus nonrandom mating. *Evol. Int. J. Org. Evol.* **57,** 2678–2687 (2003).

10. Bittles, A. H. & Neel, J. V. The costs of human inbreeding and their implications for variations at the DNA level. *Nat. Genet.* **8,** 117–121 (1994).

11. Jorde, L. B. Consanguinity and prereproductive mortality in the Utah Mormon population. *Hum. Hered.* **52,** 61–65 (2001).

12. Ober, C., Hyslop, T. & Hauck, W. W. Inbreeding effects on fertility in humans: evidence for reproductive compensation. *Am. J. Hum. Genet.* **64,** 225–231 (1999).

13. Postma, E., Martini, L. & Martini, P. Inbred women in a small and isolated Swiss village have fewer children. *J. Evol. Biol.* **23,** 1468–1474 (2010).

14. Rudan, I. *et al.* Inbreeding and risk of late onset complex disease. *J. Med. Genet.* **40,** 925–932 (2003).

15. Facon, B. *et al.* Inbreeding depression is purged in the invasive insect Harmonia axyridis. *Curr. Biol. CB* **21,** 424–427 (2011).

16. Xue, Y. *et al.* Mountain gorilla genomes reveal the impact of long-term population decline and inbreeding. *Science* **348,** 242–245 (2015).

17. Bittles, A. H., Mason, W. M., Greene, J. & Rao, N. A. Reproductive behavior and health in consanguineous marriages. *Science* **252,** 789–794 (1991).

18. Helgason, A., Pálsson, S., Gudbjartsson, D. F., Kristjánsson, T. & Stefánsson, K. An association between the kinship and fertility of human couples. *Science* **319,** 813–816 (2008).

19. Colonna, V. *et al.* Small effective population size and genetic homogeneity in the Val Borbera isolate. *Eur. J. Hum. Genet.* **21,** 89–94 (2013).

20. Esko, T. *et al.* Genetic characterization of northeastern Italian population isolates in the context of broader European genetic diversity. *Eur. J. Hum. Genet.* **21,** 659–665 (2013).

21. Traglia, M. *et al.* Heritability and demographic analyses in the large isolated population of Val Borbera suggest advantages in mapping complex traits genes. *PloS One* **4,** e7554 (2009).

22. Consortium, T. 1000 G. P. A map of human genome variation from population-scale sequencing. *Nature* **467,** 1061–1073 (2010).

23. 1000 Genomes Project Consortium *et al.* An integrated map of genetic variation from 1,092 human genomes. *Nature* **491,** 56–65 (2012).

24. Milani, G. *et al.* Computer-based genealogy reconstruction in founder populations. *J. Biomed. Inform.* **44,** 997–1003 (2011).

25. Pemberton, T. J. *et al.* Genomic patterns of homozygosity in worldwide human populations. *Am. J. Hum. Genet.* **91,** 275–292 (2012).

26. Palamara, P. F., Lencz, T., Darvasi, A. & Pe'er, I. Length Distributions of Identity by Descent Reveal Fine-Scale Demographic History. *Am. J. Hum. Genet.* **91,** 809–822 (2012).

27. Keinan, A. & Clark, A. G. Recent Explosive Human Population Growth Has Resulted in an Excess of Rare Genetic Variants. *Science* **336,** 740–743 (2012).

28. Coventry, A. *et al.* Deep resequencing reveals excess rare recent variants consistent with explosive population growth. *Nat. Commun.* **1,** 131 (2010).

29. MacArthur, D. G. *et al.* A systematic survey of loss-of-function variants in human protein-coding genes. *Science* **335,** 823–828 (2012).

30. Lawrie, D. S., Messer, P. W., Hershberg, R. & Petrov, D. A. Strong purifying selection at synonymous sites in D. melanogaster. *PLoS Genet.* **9,** e1003527 (2013).

31. Li, H. *et al.* The Sequence Alignment/Map format and SAMtools. *Bioinforma. Oxf. Engl.* **25,** 2078–2079 (2009).

32. DePristo, M. A. *et al.* A framework for variation discovery and genotyping using next-generation DNA sequencing data. *Nat. Genet.* **43,** 491–498 (2011).

33. Browning, S. R. & Browning, B. L. Rapid and Accurate Haplotype Phasing and Missing-Data Inference for Whole-Genome Association Studies By Use of Localized Haplotype Clustering. *Am. J. Hum. Genet.* **81,** 1084–1097 (2007).

34. Delaneau, O., Howie, B., Cox, A. J., Zagury, J.-F. & Marchini, J. Haplotype Estimation Using Sequencing Reads. *Am. J. Hum. Genet.* **93,** 687–696 (2013).

35. Howie, B. N., Donnelly, P. & Marchini, J. A Flexible and Accurate Genotype Imputation Method for the Next Generation of Genome-Wide Association Studies. *PLoS Genet* **5,** e1000529 (2009).

36. Howie, B., Marchini, J. & Stephens, M. Genotype Imputation with Thousands of Genomes. *G3 Genes Genomes Genet.* **1,** 457–470 (2011).

37. Sherry, S. T. *et al.* dbSNP: the NCBI database of genetic variation. *Nucleic Acids Res.* **29,** 308–311 (2001).

38. McLaren, W. *et al.* Deriving the consequences of genomic variants with the Ensembl API and SNP Effect Predictor. *Bioinforma. Oxf. Engl.* **26,** 2069–2070 (2010).

39. Wang, Y., Lu, J., Yu, J., Gibbs, R. A. & Yu, F. An integrative variant analysis pipeline for accurate genotype/haplotype inference in population NGS data. *Genome Res.* **23,** 833–842 (2013).

40. Alexander, D. H., Novembre, J. & Lange, K. Fast model-based estimation of ancestry in unrelated individuals. *Genome Res.* **19,** 1655–1664 (2009).

41. Patterson, N., Price, A. L. & Reich, D. Population structure and eigenanalysis. *PLoS Genet.* **2,** e190 (2006).

42. Sinnwell, J. P., Therneau, T. M. & Schaid, D. J. The kinship2 R package for pedigree data. *Hum. Hered.* **78,** 91–93 (2014).

43. Manichaikul, A. *et al.* Robust relationship inference in genome-wide association studies. *Bioinformatics* **26,** 2867–2873 (2010).

44. Browning, B. L. & Browning, S. R. Improving the Accuracy and Efficiency of Identity-by-Descent Detection in Population Data. *Genetics* **194,** 459–471 (2013).

45. The Genome of the Netherlands Consortium. Whole-genome sequence variation, population structure and demographic history of the Dutch population. *Nat. Genet.* **46,** 818–825 (2014).

46. Gusev, A. *et al.* Whole population, genome-wide mapping of hidden relatedness. *Genome Res.* **19,** 318–326 (2009).

47. Fenner, J. N. Cross-cultural estimation of the human generation interval for use in genetics-based population divergence studies. *Am. J. Phys. Anthropol.* **128,** 415–423 (2005).

48. Busing, F. M. T. A., Meijer, E. & Leeden, R. V. D. Delete-m Jackknife for Unequal m. *Stat. Comput.* **9,** 3–8 (1999).

49. Messer, P. W. SLiM: simulating evolution with selection and linkage. *Genetics* **194,** 1037–1039 (2013).

50. Sakharkar, M. K., Chow, V. T. K. & Kangueane, P. Distributions of exons and introns in the human genome. *In Silico Biol.* **4,** 387–393 (2004).

51. Gravel, S. *et al.* Demographic history and rare allele sharing among human populations. *Proc. Natl. Acad. Sci. U. S. A.* **108,** 11983–11988 (2011).

415–423 (2005).

Acknowledgements

Author contributions

MC, MP, PFP, EG and VC designed and performed analyses. MT, CFS, SU performed genotype quality controls. YM, RD generated and analysed exome data.

720 AKK coordinated exome sequencing/data generation. PG, DT discussed the analyses' results. NS and VC wrote the manuscript.

Competing financial interests

The authors declare no competing financial interests.

Figure Captions

725 Figure 1 - **Geographical origin of the population and evidence for systematic consanguinity in the isolated populations. (a)** Geographic location of the populations in this study. Circles are proportional to sample sizes. VBI = Val Borbera, CAR = Carlantino, FVG = Friuli Venezia Giulia, FVG-E = Erto, FVG-I = Illegio, FVG-R = Resia and FVG-S = Sauris. The figure was drawn using GNU Image Manipulation Program using maps available in the public domain. **(b)** Boxplots of genome-based

730 kinship distributions. In each population we measured genomic kinship for all possible pairs derived from: (i) all individuals ("All"); (ii) all individuals after removing one individual per pair in pairs related to 1st degree ("All Unrelated"); (iii) 46 random individuals after checking that they were not related to 1st degree in isolates. The category "All Unrelated" is empty for CEU and TSI, as there were no pairs related to 1st degree in these populations. Grey dashed lines represent reference values for

735 1st-, 2nd- and 3rd-degree relationships. Dark and light blue * and § indicate significance in comparisons with CEU and TSI, respectively (p-values in Table S5). Individuals in isolates tend to be more consanguineous than reference populations. In FVG-R and VBI relatedness to 1st degree persists even after removing 1st degree relatives according to pedigree data. The explanation is that

740   ancestors of some 2nd and 3rd degree relatives were in turn the results of consanguineous relationship, consistent with long term consanguinity in isolates.

Figure 2 - **Higher genome sharing between individuals and within individual in isolates compared to outbred reference populations.** Summary statistics **(a and b)** and cumulative frequency **(c and d)** of the total length of segments identical by descent (IBD) per pairs of individuals and total length of

745   runs of homozygosity (ROH) per single individual. In both (c) and (d) the dashed line indicates the 95% percentile. Considering an accessible genome size of 2.5Gb, individuals in FVG villages share between 13% and 18% of their genomes, versus 5-6% in other populations (c) and 5-8% of the genome in is in homozygosity in isolates (except CAR) compared to 3-4% in CEU, TSI (d).

750   Figure 3 - **Isolates experienced more genetic drift compared to reference populations**. Trends of the effective population size in the last 3000 years inferred from identical by descent genome of individuals within populations. In the last fifty generations (last ~1500 years) there was a population size contraction in FVG villages compared to CEU and TSI, which appear unaffected by the very recent trends towards expansion of other European populations. VBI and CAR instead follow the

755   trend of CEU and TSI but with substantial smaller effective population size.

Figure 4 - **Depletion in the isolates of homozygous genotypes at missense and loss of function (LoF) variants. (a)** Counts of derived allele per individual at variable sites with intergenic, synonymous, missense and LoF consequences. Statistically significant comparisons (p-value<0.001, Table S7) of
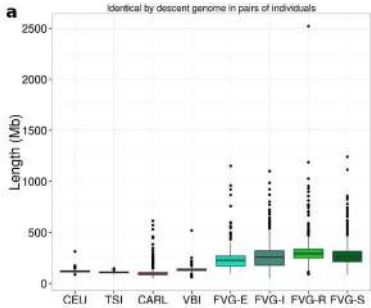
760 isolates with CEU and TSI are marked by dark and light blue asterisks, respectively. In the isolates individuals have less derived alleles compared to reference populations at intergenic and synonymous sites. **(b)** Fraction of genotypes homozygous for the derived allele at the same functional categories as in (a). At intergenic and synonymous sites isolates have significantly higher rates of homozygosity compared to reference populations (Table S7) whereas at missense and LoF

765 sites rates are comparable, suggesting a depletion of homozygous deleterious genotypes in isolates.

Figure 5 - **Isolates have less missense alleles compared to reference populations.** Pairwise comparison of isolates with CEU **(a)** and TSI **(b)** at missense, synonymous and LoF sites. RX/Y is a measure of the accumulation of mutations in population X respect to population Y; values lower than 1 indicate a depletion in population X and viceversa. Bars represent variance obtained from

770 block jackknifes. While for intergenic sites RX/Y is almost always significantly equal to 1, at other categories it is often significantly <1 suggesting more efficient selection in isolates compared to reference population. Possible causes are the founder effect, the genetic drift and the purging effect of inbreeding alongside strong selection coefficients for highly disruptive mutations. At LoF sites RX/Y are not significantly different from one, however for LoF RX/Y values were less accurate,

775 because of the low number of sites considered compared to other categories.

Figure 6 - **No contribution of the inbreeding to the depletion of deleterious mutations according to simulated results.** Purging is measured as the fold change between present and past (at founding event) average number of recessive deleterious homozygous genotypes per individual. A negative fold change is expected in case of purging. Boxplots summarize results of 100 replicates, each

780 replicate being the average over 50 individuals. Dominant, additive and recessive models are shown for neutral (selection coefficient, s=0), mildly deleterious (s=0.01) and highly deleterious (s=0.1) variants in three populations with different average kinship. Ne=effective population size.
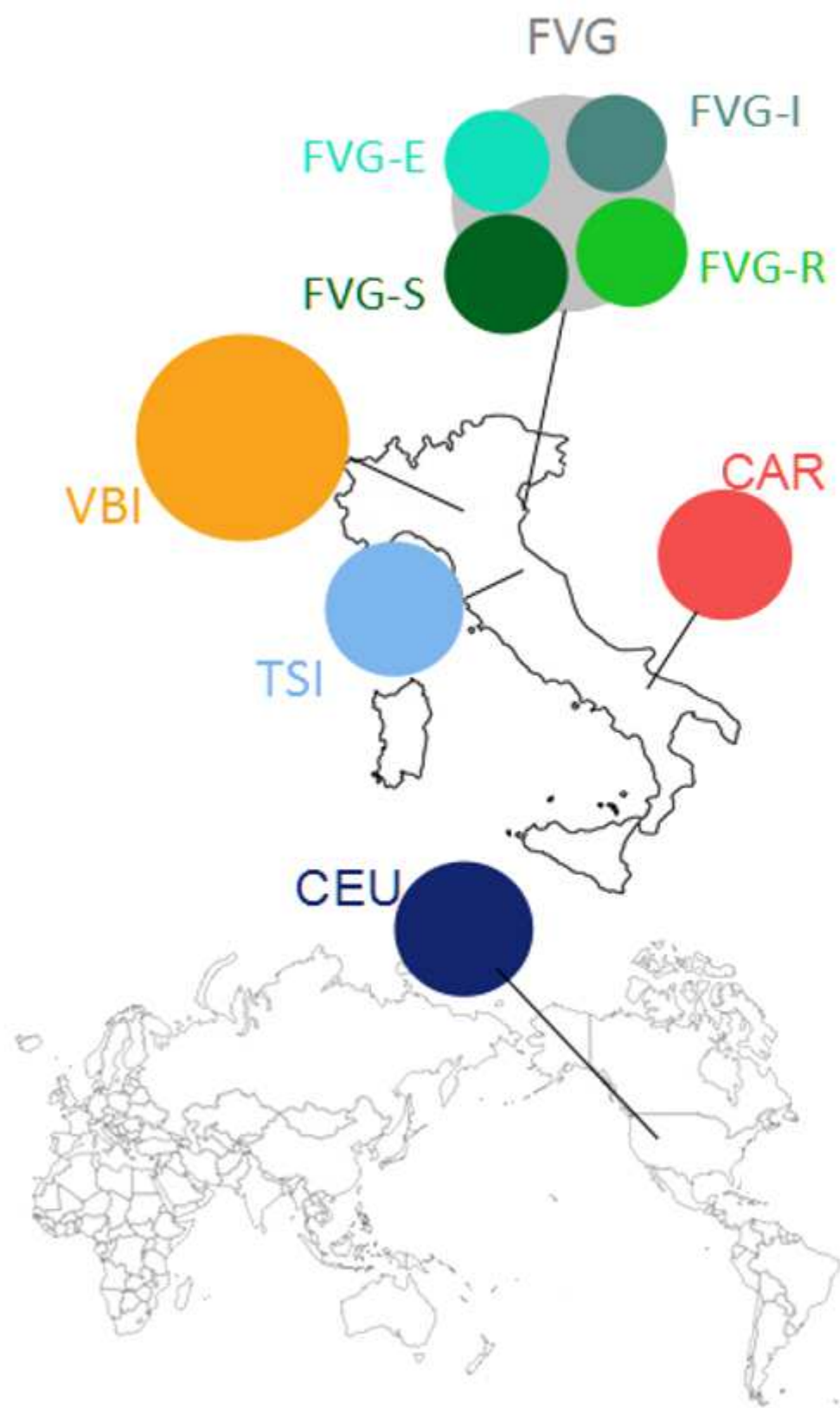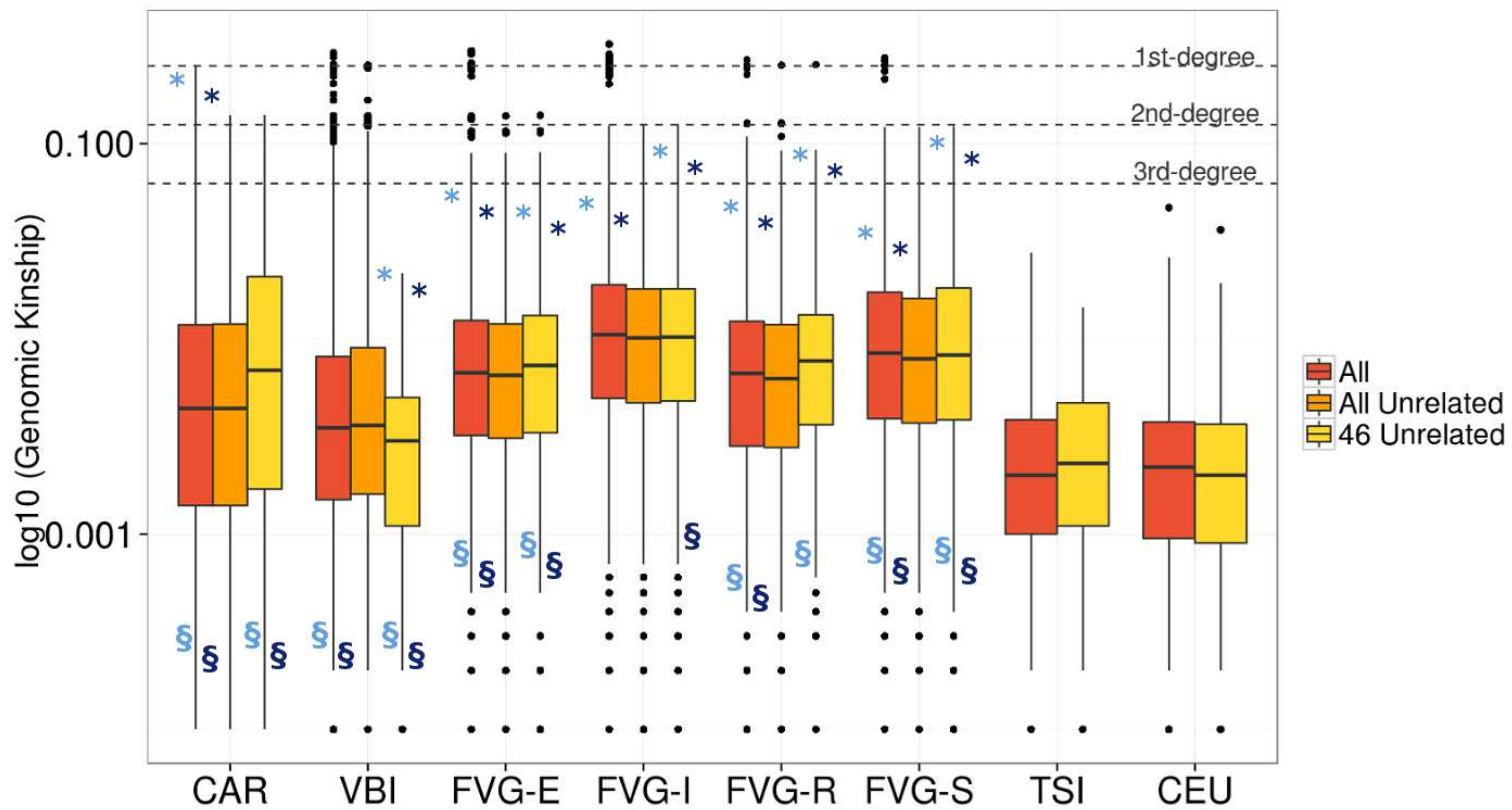
a Identical by descent genome in pairs of individuals

b Total Runs of homozygosity per individual

d

c

Cohorts
- CEU
- TSI
- CAR
- VBI
- FVG-E
- FVG-I
- FVG-R
- FVG-S